



1 **Twin-plate ice nucleation assay (TINA) with infrared detection for**  
2 **high-throughput droplet freezing experiments with biological ice**  
3 **nuclei in laboratory and field samples**

4

5 **Anna T. Kunert<sup>1</sup>, Mark Lamneck<sup>2</sup>, Frank Helleis<sup>2</sup>, Mira L. Pöhlker<sup>1</sup>, Ulrich Pöschl<sup>1</sup>, and**  
6 **Janine Fröhlich-Nowoisky<sup>1,\*</sup>**

7

8 <sup>1</sup>Multiphase Chemistry Department, Max Planck Institute for Chemistry, 55128 Mainz,  
9 Germany

10 <sup>2</sup>Instrument Development and Electronics, Max Planck Institute for Chemistry, 55128 Mainz,  
11 Germany

12

13 *Correspondence to:* Janine Fröhlich-Nowoisky ([j.frohlich@mpic.de](mailto:j.frohlich@mpic.de))



14 **Abstract.** For efficient analysis and characterization of biological ice nuclei under immersion  
15 freezing conditions, we developed a Twin-plate Ice Nucleation Assay (TINA) for high-  
16 throughput droplet freezing experiments, in which the temperature gradient and freezing of  
17 each droplet is tracked by an infrared detector. In the fully automated setup, a couple of  
18 independently cooled aluminum blocks carrying two 96-well plates and two 384-well plates,  
19 respectively, are available to study ice nucleation and freezing events simultaneously in  
20 hundreds of microliter range droplets (0.1-40  $\mu\text{L}$ ). A cooling system with two refrigerant  
21 circulation loops is used for high-precision temperature control (deviations  $<0.5$  K), enabling  
22 measurements over a wide range of temperatures ( $\sim 233$ - $270$  K) at variable cooling rates (up to  
23  $10$  K  $\text{min}^{-1}$  and more).

24 The TINA instrument was tested and characterized in experiments with bacterial and  
25 fungal ice nuclei (IN) from *Pseudomonas syringae* (Snomax<sup>®</sup>) and *Mortierella alpina*,  
26 exhibiting freezing curves in good agreement with literature data. Moreover, TINA was applied  
27 to investigate the influence of chemical processing on the activity of biological IN, in particular  
28 the effects of oxidation and nitration reactions. Upon exposure of Snomax<sup>®</sup> samples to  $\text{O}_3$  and  
29  $\text{NO}_2$ , the concentration of IN active around 269 K ( $-4$  °C, “class A”) decreased by about two  
30 orders of magnitude, while the concentration of IN active around 265 K ( $-8$  °C, “class C”)   
31 decreased by about one order of magnitude. Furthermore, TINA was used to study aqueous  
32 extracts of atmospheric aerosols, simultaneously investigating a multitude of samples that were  
33 treated in different ways to distinguish different kinds of IN. For example, heat treatment and  
34 filtration experiments indicated that highly efficient biological IN were smaller than  $0.1$   $\mu\text{m}$ ,  
35 and many IN active between 263 K ( $-10$  °C) and 256 K ( $-14$  °C) were heat-resistant and larger  
36 than  $5$   $\mu\text{m}$ . The results confirm that TINA is suitable for high-throughput experiments and  
37 efficient analysis of biological IN in laboratory and field samples.



## 38 **1 Introduction**

39 Clouds and aerosols still contribute the largest uncertainty to the evaluation of the Earth's  
40 changing energy budget (Boucher et al., 2013). Thus, the understanding of the contribution of  
41 atmospheric aerosols in cloud processes is of fundamental importance. Atmospheric ice  
42 nucleation is essential for cloud glaciation and precipitation, thereby influencing the  
43 hydrological cycle and climate. Ice can be formed via homogeneous nucleation in liquid water  
44 droplets or heterogeneous nucleation triggered by particles serving as atmospheric ice nuclei  
45 (IN) (Pruppacher and Klett, 1997).

46 A wide range of droplet freezing assays and instruments have been developed and  
47 applied for the analysis of IN in immersion freezing experiments (e.g., Budke and Koop, 2015;  
48 Fröhlich-Nowoisky et al., 2015; Häusler et al., 2018; Murray et al., 2010; O'Sullivan et al.,  
49 2014; Stopelli et al., 2014; Tobo, 2016; Vali, 1971b, 1971a; Whale et al., 2015; Wright and  
50 Petters, 2013; Zarogotas et al., 2016). Most of the available assays and instruments, however,  
51 are limited to the investigation of small droplet numbers and use optical detection systems in  
52 the UV/Vis wavelength range. As shown by Zarogotas et al. (2016), however, infrared (IR)  
53 detector enable improved detection of droplet freezing.

54 Upon the phase change of water from liquid to solid, latent heat is released resulting in  
55 a sudden temperature change of the droplet, which can be detected by infrared (IR) video  
56 thermography. In 1995, Ceccardi et al. (1995) used IR video thermography as a new technique  
57 to non-destructively study ice formation on plants by visualizing the changes in surface  
58 temperature. Wisniewski et al. (1997) evaluated the IR video thermography under controlled  
59 conditions and determined it as an excellent method for directly observing ice nucleation and  
60 propagation in plants. Since then, IR video thermography was used in a range of studies  
61 investigating freezing in plants (e.g., Ball et al., 2002; Carter et al., 1999; Charrier et al., 2017;  
62 Fuller and Wisniewski, 1998; Hacker and Neuner, 2007; Pearce and Fuller, 2001; Sekozawa et  
63 al., 2004; Stier et al., 2003; Wisniewski et al., 2008; Workmaster, 1999). Further applications  
64 of IR video thermography are investigations of cold thermal stress in insects (Gallego et al.,  
65 2016), monitoring of freeze drying processes (Emteborg et al., 2014), detection of ice in wind  
66 turbine blades (Gómez Muñoz et al., 2016) and helicopter rotor blades (Hansman and  
67 Dershowitz, 1994). Freezing of single water droplets in an acoustic levitator has also been  
68 successfully observed by IR video thermography (Bauerecker et al., 2008).

69 Here, we introduce a Twin-plate Ice Nucleation Assay (TINA) for high-throughput  
70 droplet freezing experiments in which the temperature gradient and freezing of each droplet is  
71 tracked by an infrared detector. In the fully automated setup, a couple of independently cooled



72 aluminum blocks carrying two 96-well and two 384-well plastic plates, respectively, are  
73 available to study ice nucleation and freezing events in nearly 1000 microliter range droplets  
74 simultaneously. A cooling system with two refrigerant circulation loops is used for high-  
75 precision temperature control (deviations  $<0.5$  K), enabling measurements over a wide range  
76 of temperatures ( $\sim 233$ - $270$  K ( $\sim -50$  °C to  $-3$  °C)) at variable cooling rates (up to  $10$  K  $\text{min}^{-1}$   
77 and more). The instrument was developed in the course of the INUIT project over the last three  
78 years, in which it has been presented and discussed at several conferences and workshops  
79 (Kunert et al., 2016a, 2016b, 2017a, 2017b, 2018). We use the bacterial IN Snomax<sup>®</sup> and the  
80 IN-active fungus *Mortierella alpina* as biological test substances to investigate heterogeneous  
81 ice nucleation. Moreover, TINA is applied to investigate the effect of O<sub>3</sub> and NO<sub>2</sub> exposure on  
82 the IN activity of Snomax<sup>®</sup>. Furthermore, aqueous extracts of atmospheric aerosols are treated  
83 in different ways and are analyzed for different kinds of IN. Very recently, a similar approach  
84 for droplet freezing experiments with IR detection has been presented by Harrison et al. (2018),  
85 investigating K-feldspar, NX-illite, and atmospheric aerosol samples.

86

## 87 2 Experimental setup

### 88 2.1 Technical details

89 The core of the Twin-plate Ice Nucleation Assay (TINA) are two independently cooled,  
90 customized sample holder aluminum blocks, which have been shaped for multiwell plates with  
91 96 and 384 wells, respectively. In each cooling block, two multiwell plates can be analyzed  
92 simultaneously. The maximal droplet volume in the 96-well block is  $250$   $\mu\text{L}$ , and the minimal  
93 droplet volume is  $0.1$   $\mu\text{L}$ , which is the limit of our liquid handling station (epMotion ep5073,  
94 Eppendorf, Hamburg, Germany). As shown in Fig. 1, the design of the two sample holder  
95 blocks is basically identical, but the detailed construction varies slightly. Both blocks consist  
96 of two parts, a trough and a cap, which are screwed together and sealed with an O-ring. But, for  
97 the 96-well block (Fig. 1a), the trough is at the bottom (Fig. 1c) and the cap is at the top (Fig.  
98 1b), whereas, for the 384-well block (Fig. 1d), the trough is at the top (Fig. 1e) and the cap is  
99 at the bottom (Fig. 1f). Two openings with Swagelok adapters for cooling liquid are placed next  
100 to each other, and the cooling liquid flows in a small passage around an elevation in the middle  
101 of the trough.

102 The customized sample holder blocks are cooled with a silicon-based cooling liquid  
103 (SilOil M80.055.03, Peter Huber Kältemaschinenbau AG, Offenburg, Germany) tempered by  
104 an external high-performance refrigeration bath circulator (CC-508 with Pilot ONE, Peter  
105 Huber Kältemaschinenbau AG), which can supply temperatures down to  $218$  K ( $-55$  °C). Both



106 sample holder blocks can be operated in parallel and independently from each other due to the  
107 usage of two self-developed mixing valves and cooling loops (Fig. 2). This allows either the  
108 cooling of two different droplet freezing assays at the same time, or the observation of 960  
109 droplets in one experiment. The mixing of a cold and a warm loop of cooling liquid for each  
110 block enables a fast and precise adjustment of the sample holder block temperatures without  
111 being dependent on the cooling rate of the refrigeration bath circulator itself. In each  
112 experiment, the refrigeration bath circulator is cooled down 5 K below the coldest temperature,  
113 which is projected for the experiment, while no mixing of warm and cold cooling liquid occurs.  
114 By changing the position of the mixing valves for a defined period of time, cold and warm  
115 cooling liquids are mixed together, so that the desired temperatures within the two blocks are  
116 reached. Two pumps (VPP-655 PWM Single Version, Alphacool International GmbH,  
117 Braunschweig, Germany) ensure the continuous circulation of cooling liquid through each  
118 block independently from the position of the mixing valves. Figure 3 is a schematic illustration  
119 of the overall setup of TINA.

120

## 121 2.2 Temperature control and calibration

122 Within each sample holder block, the temperature is measured with two temperature sensors, a  
123 NTC thermistor in the cooling liquid stream (TH-44033, resistance: 2255  $\Omega$ /298 K,  
124 interchangeability:  $\pm 0.1$  K, Omega Engineering GmbH, Deckenpfronn, Germany) and a  
125 customized NTC thermistor (10K3MRBD1, resistance: 10000  $\Omega$ /298 K, interchangeability:  
126  $\pm 0.2$  K, TE Connectivity Company, Galway, Ireland) in the elevation. Another NTC thermistor  
127 (10K3MRBD1, resistance: 10000  $\Omega$ /298 K, interchangeability:  $\pm 0.2$  K, TE Connectivity  
128 Company) monitors the temperature behind each mixing valve. Temperature control within the  
129 entire system is achieved by a self-developed microcontroller-based electronic system. The  
130 analog input unit is equipped with a 24 Bit Low Noise Delta-Sigma ADC (ADS1256), which  
131 assures the required accuracy to process the resolution of the used thermistors. All thermistors  
132 had been calibrated with a reference thermometer (2180A, resolution: 0.01 K, maximum system  
133 error:  $\pm 0.08$  K at 223 K and  $\pm 0.07$  K at 273 K, Fluke Deutschland GmbH, Glottertal,  
134 Germany). Therefore, all thermistors were bound together with a PT100 sensor of the reference  
135 thermometer, and the bundle was placed inside a brass cylinder filled with cooling liquid. The  
136 cylinder was placed inside the cooling bath of the refrigeration bath circulator. The temperature  
137 within the bath was cooled down from 303.2 K to 218.2 K (30.0  $^{\circ}$ C to -55.0  $^{\circ}$ C) in 5 K steps  
138 and raised again from 220.7 K to 300.7 K (-52.5  $^{\circ}$ C to 27.5  $^{\circ}$ C) in 5 K steps. Each step was kept  
139 for 30 min to equilibrate the temperature, while the resistance of all thermistors and the



140 temperature measured by the reference thermometer were monitored. For the conversion of the  
141 measured resistance of the thermistors into temperature, cubic spline interpolation was used.

142

### 143 **2.3 Infrared video thermography**

144 Droplet freezing is determined by a distinct detection system, where the temperature gradient  
145 of each single droplet is tracked by infrared cameras (Seek Thermal Compact XR, Seek  
146 Thermal Inc., Santa Barbara, CA, USA) coupled to a self-written software. This concept  
147 enables a doubtless determination of freezing events because freezing of supercooled liquid  
148 releases energy, which leads to an abrupt rise in the detected temperature of the observed  
149 droplet, as discussed earlier (Sect. 1). This detection system uses the IR video thermography  
150 only to determine freezing events, while the proper temperature is monitored by thermistors. In  
151 contrast, Zaragotas et al. (2016) used infrared camera, which was calibrated only once by the  
152 company, to measure the accurate temperature of each droplet. Figure 4 is a sequence of  
153 infrared camera images showing 384 droplets during cooling and freezing (red circles).  
154 Software analysis uses a grid of 96 and 384 points, respectively, where the grid point is set to  
155 the center of each well enabling to fit the dimensions of each plate under different perspective  
156 angles. The temperature gradient is tracked for each well during the experiment. A self-written  
157 algorithm detects a local maximum shortly followed by a local minimum in the derivative of  
158 the temperature profile, which is caused by the release of latent heat during freezing. The  
159 software exports the data for each droplet in CSV format.

160

### 161 **2.4 Data analysis**

162 Assuming ice nucleation as a time-independent (singular) process, the concentration of IN ( $n_m$ )  
163 active at a certain temperature ( $T$ ) per unit mass of material is given by Eq. (1) (Vali, 1971a).

$$164 \quad n_m(T) = \frac{-\ln(1-f_{ice})}{V_{drop}} \cdot \frac{d}{m} \quad (1)$$

165 where  $f_{ice}$  is the fraction of frozen droplets at a particular temperature,  $V_{drop}$  the droplet volume,  
166  $m$  the mass of the particles in the initial suspension, and  $d$  the dilution factor of the droplets  
167 relative to  $m$ . To simplify data analysis, freezing events were merged in 0.1 K bins.

168

### 169 **3. Freezing experiments**

170 The fully automated TINA setup was tested and characterized for immersion freezing  
171 experiments with pure water droplets, as well as Snomax<sup>®</sup> and IN filtrate of the fungus  
172 *Mortierella alpina* as biological reference substances. Moreover, TINA was used to study the



173 effect of O<sub>3</sub> and NO<sub>2</sub> exposure on the IN activity of Snomax<sup>®</sup>. Furthermore, TINA was applied  
174 to atmospheric aerosol samples.

175

### 176 3.1 Pure water

177 Pure water was obtained from a Barnstead<sup>™</sup> GenPure<sup>™</sup> xCAD Plus water purification system  
178 (Thermo Scientific, Braunschweig, Germany). The water was autoclaved at 394 K (121 °C) for  
179 20 min, filtered three times through a sterile 0.1 μm pore diameter sterile polyethersulfone  
180 (PES) vacuum filter unit (VWR International, Radnor, PA, USA), and autoclaved again.

181 For background measurements, 3 μL aliquots of autoclaved and filtered pure water were  
182 pipetted into 96-well plates (Axon Labor Technik, Kaiserslautern, Germany) and 384-well plates  
183 (Eppendorf), respectively, by a liquid handling station. Therefore, four (96-well plate) and eight  
184 (384-well plate) different water samples were pipetted column-wise distributed into the plates.  
185 In total, six columns per sample were apportioned over the two twin-plates, i.e., 48 droplets per  
186 sample in 96-well plates, and 96 droplets per sample in 384-well plates. The plates were placed  
187 in the sample holder blocks and were cooled down quickly to 273 K (0 °C), and, as soon as the  
188 temperature was stable for one minute, in a continuous cooling rate of 1 K min<sup>-1</sup> further down  
189 to 238 K (-35 °C).

190 As the phase transition from liquid water to ice is kinetically hindered, supercooled  
191 water can stay liquid at temperatures down to 235 K (-38 °C), where homogeneous ice  
192 nucleation takes place. This is only true for nanometer-sized droplets because the freezing  
193 temperature is dependent on droplet volume and cooling rate, and the classical nucleation  
194 theory predicts a homogeneous freezing temperature of about 240 K (-33 °C) for microliter  
195 volume droplets using a cooling rate of 1 K min<sup>-1</sup> (Fornea et al., 2009; Murray et al., 2010;  
196 Pruppacher and Klett, 1997; Tobo, 2016). However, several studies have reported average  
197 freezing temperatures for microliter volume droplets of pure water at significantly warmer  
198 subfreezing temperatures due to possible artifacts (e.g., Conen et al., 2011; Fröhlich-Nowoisky  
199 et al., 2015; Hill et al., 2016; Whale et al., 2015). To our knowledge, only two studies reported  
200 an average homogeneous freezing temperature of 240 K (-33 °C) for microliter volume droplets  
201 and a cooling rate of 1 K min<sup>-1</sup>, using hydrophobic surfaces as contact area for the droplets  
202 (Fornea et al., 2009; Tobo, 2016). Providing microliter droplets free of suspended IN and  
203 surfaces free of contaminants is difficult, so that the temperature limit below which freezing  
204 cannot be traced back to heterogeneous IN needs to be determined individually for each setup.

205 Our results show that most pure water droplets froze around 247 K (-26 °C) in 96-well  
206 plates (Fig. 5a) and around 244 K (-29 °C) in 384-well plates (Fig. 5b), respectively. This



207 discrepancy can have different explanations. First, the 96-well plates are obtained from a  
208 different manufacturer than the 384-well plates. Second, the different well shape leads to an  
209 altered shape of the droplet, which could influence its freezing abilities at very low  
210 temperatures. All in all, these freezing temperatures are substantially above the expected  
211 temperatures for homogeneous nucleation of microliter droplets, but they are in accord with the  
212 results of Whale et al. (2015).

213

### 214 **3.2 Biological reference materials**

215 The performance of TINA was further assessed using Snomax<sup>®</sup> as a bacterial IN-active  
216 reference substance (e.g., Budke and Koop, 2015; Hartmann et al., 2013; Möhler et al., 2008;  
217 Turner et al., 1990; Ward and DeMott, 1989) and IN filtrate of the well-studied IN fungus  
218 *Mortierella alpina* (Fröhlich-Nowoisky et al., 2015; Pummer et al., 2015).

219 Snomax<sup>®</sup> was obtained from SMI Snow Makers AG (Thun, Switzerland), and a stock  
220 solution was prepared in pure water with an initial mass concentration of 1 mg mL<sup>-1</sup>. This  
221 suspension was then serially diluted 10-fold with pure water by the liquid handling station. The  
222 resulting Snomax<sup>®</sup> concentrations varied between 1 mg mL<sup>-1</sup> and 0.1 ng mL<sup>-1</sup>, equivalent to a  
223 total mass of Snomax<sup>®</sup> between 3 µg and 0.3 pg, respectively, per 3 µL droplet.

224 Each dilution was pipetted column-wise distributed over the twin-plates as described  
225 before in 96 droplets into 384-well plates by the liquid handling station. Two plates at a time  
226 were placed inside the 384-well sample holder block, and the plates were cooled down quickly  
227 to 273 K (0 °C), and, as soon as the temperature was stable for one minute, in a continuous  
228 cooling rate of 1 K min<sup>-1</sup> further down to 253 K (-20 °C).

229 Three independent experiments with Snomax<sup>®</sup> show reproducible results (Fig. S1).  
230 Therefore, droplets of the same dilution were added to a total droplet number of 288 (Fig. 6a).  
231 The data show two strong increases in the cumulative number of IN, one around 269 K (-4 °C)  
232 and one around 265 K (-8 °C), interrupted by a slightly increasing plateau between 268 K and  
233 266 K (-5 °C and -7 °C). These differences result from three different classes of IN with  
234 different activation temperatures as described by Turner et al. (1990). Based on this  
235 classification, the Snomax<sup>®</sup> sample contains a large number of class A and C IN, but only a few  
236 IN of class B. These findings are in accordance with the results of Budke and Koop (2015).  
237 Below 259 K (-14 °C), a flat plateau arises where no IN are active.

238 The analysis of different IN active within a wide temperature range was only possible  
239 due to the measurement of a dilution series. TINA enables the simultaneous measurement of  
240 such a dilution series with high statistics in a short period of time.



241 *Mortierella alpina* 13A was grown on full-strength PDA (VWR International GmbH,  
242 Darmstadt, Germany) at 269 K for 7 months. Fungal IN filtrate was prepared as described  
243 previously (Fröhlich-Nowoisky et al., 2015; Pummer et al., 2015) and contained IN from spores  
244 and mycelial surfaces. It was serially diluted 10-fold with pure water by the liquid handling  
245 station. The experiment was performed as described above.

246 For test measurements with fungal IN, IN filtrate of three different culture plates from  
247 *Mortierella alpina* 13A was measured, and the results were reproducible (Fig. S2). The  
248 cumulative number of IN per gram mycelium only varies between one order of magnitude,  
249 which is a good achievement for a biological sample, and droplets of the same dilutions were  
250 added to a total droplet number of 288 (Fig. 6b). The cumulative number of IN and the initial  
251 freezing temperature of 267.7 K (-5.5 °C) are in good agreement with the literature (Fröhlich-  
252 Nowoisky et al., 2015; Pummer et al., 2015).

253

### 254 3.3 Ozonized and nitrated samples

255 To study the effect of O<sub>3</sub> and NO<sub>2</sub> exposure on the IN activity of Snomax<sup>®</sup>, an aliquot of 1 mL  
256 of a 1 mg mL<sup>-1</sup> suspension of Snomax<sup>®</sup> in pure water was exposed in liquid phase to gases with  
257 or without O<sub>3</sub> and NO<sub>2</sub> as described in Liu et al. (2017). A dilution series of the treated samples  
258 was measured as described for the Snomax<sup>®</sup> reference measurements.

259 The results show that high concentrations of O<sub>3</sub> and NO<sub>2</sub> reduce the concentration of IN  
260 active around 269 K (-4 °C, “class A”) about two orders of magnitude, while the concentration  
261 of IN active around 265 K (-8 °C, “class C”) decreased by about one order of magnitude (Fig.  
262 7). The cumulative number of IN per unit mass is slightly reduced by the exposure to synthetic  
263 air, which can be explained by a small loss of IN within the system during exposure.

264 Snomax<sup>®</sup> contains IN proteins of the bacterium *Pseudomonas syringae*. Attard et al.,  
265 (2012) found no significant or only weak effects of exposure to ~100 ppb O<sub>3</sub> and ~100 ppb NO<sub>2</sub>  
266 on the IN activity of two strains of *P. syringae*, and a variable response of a third strain,  
267 suggesting a strain-specific response.

268

### 269 3.4 Air filter samples

270 Total suspended particle samples were collected onto 150 mm glass fiber filters (Type MN  
271 85/90, Macherey-Nagel GmbH, Düren, Germany) using a high-volume sampler (DHA-80,  
272 Digital Elektronik AG, Hegnau, Switzerland) operated at 1000 L min<sup>-1</sup>, which was placed at  
273 the roof of the Max Planck Institute for Chemistry (MPIC, Mainz, Germany). There, a mix of  
274 urban and rural continental boundary layer air can be sampled in central Europe. The filter was



275 taken in April 2018, and the sampling period was seven days, corresponding to a total air  
276 volume of approximately 10,000 m<sup>3</sup>. Filters were pre-baked at 603 K (330 °C) for 10 h to  
277 remove any biological material, and blank samples were taken to detect possible  
278 contaminations. All filters were packed in pre-baked aluminum bags, and loaded filters were  
279 stored at 193 K (-80 °C) until analysis.

280 Filters were cut with a sterilized scissor into aliquots (~1/16), and the exact percentage  
281 was determined gravimetrically. For reproducibility, aerosol and blank filter sample aliquots of  
282 each filter were extracted. Each filter sample aliquot was transferred into a sterile 50 mL tube  
283 (Greiner Bio One, Kremsmünster, Austria), and 10 mL of pure water was added. The tubes  
284 were shaken horizontally at 200 rpm for 15 min. Afterwards, the filter was removed, and the  
285 aqueous extract was tested for IN activity. To further characterize the IN, the effects of filtration  
286 and heat treatment were investigated. Therefore, aliquots of the extract were treated as follows:  
287 (i) 1 h at 371 K (98 °C), (ii) filtration through a 5 µm pore diameter filter (Acrodisc, PES, Pall,  
288 Germany), (iii) filtration through a 5 µm and a 0.1 µm pore diameter filter (Acrodisc).

289 Each solution (96 aliquots of 3 µL) was pipetted column-wise into 384-well plates by  
290 the liquid handling station. The plates were cooled down quickly to 273 K (0 °C), and, as soon  
291 as the temperature was stable for one minute, in a continuous cooling rate of 1 K min<sup>-1</sup> further  
292 down to 243 K (-30 °C).

293 Each solution of the two aliquots of each filter was measured separately, and droplets  
294 of the same solution were added to a total droplet number of 192 (2 x 96 droplets) (Fig. S3).  
295 For better clearness, data of different dilutions were averaged for each treatment (Fig. 8).

296 The untreated filter extract showed IN activity at relatively warm subfreezing  
297 temperatures with an initial freezing temperature of 267 K (-6 °C). The concentration of IN  
298 active at temperatures above 263 K (-10 °C) was about 10<sup>-3</sup> L<sup>-1</sup>, but heat treatment led to a loss  
299 of IN activity above 263 K (-10 °C), which indicates the presence of biological IN. The  
300 concentration of IN between 263 K (-10 °C) and 255 K (-18 °C) increased continuously about  
301 two orders of magnitude and in a sudden increase another two orders between 255 K (-18 °C)  
302 and 254 K (-19 °C). A maximum IN concentration of 10<sup>2</sup> L<sup>-1</sup> was reached around 250 K (-23  
303 °C), but heat treatment reduced the maximum IN concentration to 10<sup>1</sup> L<sup>-1</sup> at 250 K (-23 °C).  
304 Filtration experiments did not affect the initial freezing temperature, but the concentration of  
305 biological IN was decreased about half an order of magnitude, at which the 0.1 µm filtration  
306 showed a slightly bigger effect. The concentration of IN active between 263 K (-10 °C) and  
307 256 K (-17 °C) decreased about two orders of magnitude upon 5 µm filtration, and 0.1 µm  
308 filtration reduced the IN concentration slightly more. The maximum IN concentration of 10<sup>2</sup> L<sup>-1</sup>



309 <sup>1</sup> around 250 K (-23 °C) was not affected upon filtration. The results suggest that there were  
310 highly efficient biological IN smaller than 0.1 μm and other biological IN or agglomerates of  
311 the same biological IN with different sizes. Moreover, the findings show that many IN active  
312 between 263 K (-10 °C) and 256 K (-17 °C) were larger than 5 μm, whereas IN active between  
313 256 K (-17 °C) and 250 K (-23 °C) were smaller than 0.1 μm. Most of the IN active between  
314 263 K (-10 °C) and 259 K (-14 °C) were heat-resistant.

315 The results of both, the untreated and the heated filter extracts, showed a few outliers.  
316 These were probably caused by single large particles or aggregates larger than 5 μm, which  
317 were statistically distributed over the different dilutions. These particles nucleated at warmer  
318 subfreezing temperatures than the other IN within a dilution, so they are overestimated due to  
319 their efficient nucleation. This hypothesis is supported by the fact that the filtered filter extracts  
320 did not contain any outliers.

321

#### 322 4 Conclusions

323 The new high-throughput droplet freezing assay TINA was introduced to study heterogeneous  
324 ice nucleation of microliter range droplets in the immersion mode. TINA provides the analysis  
325 of 960 droplets simultaneously or 192 and 768 droplets in two independent experiments at the  
326 same time, enabling the analysis of many samples with high statistics in a short period of time.  
327 Moreover, an infrared camera-based detection system allows to reliably determine droplet  
328 freezing. The setup was tested with Snomax<sup>®</sup> as bacterial IN, and IN filtrate of *Mortierella*  
329 *alpina* as fungal IN. For these reference materials, both, the initial freezing temperature and the  
330 cumulative number of IN per gram mycelium, were in accordance with the literature, which  
331 demonstrates the functionality of the new setup.

332 TINA was applied to study the effect of O<sub>3</sub> and NO<sub>2</sub> exposure on the IN activity of  
333 Snomax<sup>®</sup>, where high concentrations of O<sub>3</sub> and NO<sub>2</sub> reduced the IN activity significantly.  
334 Atmospheric aerosol samples from Mainz (Germany) were analyzed for IN activity to show the  
335 applicability of TINA for field samples. Here, we found highly efficient biological IN smaller  
336 than 0.1 μm and heat-resistant IN larger than 5 μm. The results confirm that TINA is suitable  
337 for high-throughput experiments and efficient analysis of biological IN in laboratory and field  
338 samples.



339 *Author Contributions.* A.T.K., M.L., and F.H. developed the instrument. A.T.K., U.P., J.F.-N.  
340 conceived and designed the experiments. A.T.K. performed the experiments. M.L.P. wrote the  
341 code to process the data. All authors discussed the data and contributed to the writing of the  
342 manuscript.

343

344 *Competing Interests.* The authors declare that they have no conflict of interest.

345

346 *Acknowledgements.* The authors thank C. Gurk, T. Klimach, F. Kunz and the workshop team  
347 for supporting the experimental setup, N. M. Kropf, C. Krevert, I. Maurus, G. Kopper, and P.  
348 Yordanova for technical support, and H. Grothe, T. Koop, N. Lang-Yona, and J. F. Scheel for  
349 helpful discussions. The Max Planck Society (MPG) and the Ice Nuclei research Unit of the  
350 Deutsche Forschungsgemeinschaft (DFG FR 3641/1-2, FOR 1525 INUIT) are acknowledged  
351 for financial support.

352 **References**

- 353 Attard, E., Yang, H., Delort, A. M., Amato, P., Pöschl, U., Glaux, C., Koop, T. and Morris, C.  
354 E.: Effects of atmospheric conditions on ice nucleation activity of *Pseudomonas*, *Atmos. Chem.*  
355 *Phys.*, 12(22), 10667–10677, doi:10.5194/acp-12-10667-2012, 2012.
- 356 Ball, M. C., Wolfe, J., Canny, M., Hofmann, M., Nicotra, A. B. and Hughes, D.: Space and  
357 time dependence of temperature and freezing in evergreen leaves, *Funct. Plant. Biol.*, 29, 1259–  
358 1272, 2002.
- 359 Bauerecker, S., Ulbig, P., Buch, V., Vrbka, L. and Jungwirth, P.: Monitoring ice nucleation in  
360 pure and salty water via high-speed imaging and computer simulations, *J. Phys. Chem. C*,  
361 112(20), 7631–7636, doi:10.1021/jp711507f, 2008.
- 362 Boucher, O., Randall, D., Artaxo, P., Bretherton, C., Feingold, G., Forster, P., Kerminen, V.-  
363 M., Kondo, Y., Liao, H., Lohmann, U., Rasch, P., Satheesh, S. K., Sherwood, S., Stevens, B.  
364 and Zhang, X. Y.: Clouds and Aerosols, in *Climate Change 2013: The Physical Science Basis.*  
365 *Contribution of Working Group I to the Fifth Assessment Report of the Intergovernmental*  
366 *Panel on Climate Change*, edited by T. F. Stocker, D. Qin, G.-K. Plattner, M. Tignor, S. K.  
367 Allen, J. Boschung, A. Nauels, Y. Xia, V. B. And, and P. M. Midgley, pp. 571–657, Cambridge  
368 University Press, Cambridge, United Kingdom and New York, NY, USA., 2013.
- 369 Budke, C. and Koop, T.: BINARY: an optical freezing array for assessing temperature and time  
370 dependence of heterogeneous ice nucleation, *Atmos. Meas. Tech.*, 8(2), 689–703,  
371 doi:10.5194/amt-8-689-2015, 2015.
- 372 Carter, J., Brennan, R. and Wisniewski, M.: Low-temperature tolerance of blackcurrant flowers,  
373 *HortScience*, 34(5), 855–859, 1999.
- 374 Ceccardi, T. L., Heath, R. L. and Ting, I. P.: Low-temperature exotherm measurement using  
375 infrared thermography, *HortScience*, 30(1), 140–142, 1995.
- 376 Charrier, G., Nolf, M., Leitinger, G., Charra-Vaskou, K., Losso, A., Tappeiner, U., Améglio,  
377 T. and Mayr, S.: Monitoring of Freezing Dynamics in Trees: A Simple Phase Shift Causes  
378 Complexity, *Plant Physiol.*, 173(4), 2196–2207, doi:10.1104/pp.16.01815, 2017.
- 379 Conen, F., Morris, C. E., Leifeld, J., Yakutin, M. V. and Alewell, C.: Biological residues define  
380 the ice nucleation properties of soil dust, *Atmos. Chem. Phys.*, 11(18), 9643–9648,  
381 doi:10.5194/acp-11-9643-2011, 2011.
- 382 Emteborg, H., Zeleny, R., Charoud-Got, J., Martos, G., Lüddecke, J., Schellin, H. and Teipel,  
383 K.: Infrared thermography for monitoring of freeze-drying processes: Instrumental  
384 developments and preliminary results, *J. Pharm. Sci.*, 103(7), 2088–2097,  
385 doi:10.1002/jps.24017, 2014.



- 386 Fornea, A. P., Brooks, S. D., Dooley, J. B. and Saha, A.: Heterogeneous freezing of ice on  
387 atmospheric aerosols containing ash, soot, and soil, *J. Geophys. Res. Atmos.*, 114(13), 1–12,  
388 doi:10.1029/2009JD011958, 2009.
- 389 Fröhlich-Nowoisky, J., Hill, T. C. J., Pummer, B. G., Yordanova, P., Franc, G. D. and Pöschl,  
390 U.: Ice nucleation activity in the widespread soil fungi *Mortierella alpina*, *Biogeosciences*, 12,  
391 1057–1071, doi:10.5194/bg-12-1057-2015, 2015.
- 392 Fuller, M. . and Wisniewski, M.: The use of infrared thermal imaging in the study of ice  
393 nucleation and freezing of plants, *J. Therm. Biol.*, 23(2), 81–89, doi:10.1016/S0306-  
394 4565(98)00013-8, 1998.
- 395 Gallego, B., Verdú, J. R., Carrascal, L. M. and Lobo, J. M.: A protocol for analysing thermal  
396 stress in insects using infrared thermography, *J. Therm. Biol.*, 56, 113–121,  
397 doi:10.1016/j.jtherbio.2015.12.006, 2016.
- 398 Gómez Muñoz, C. Q., García Márquez, F. P. and Sánchez Tomás, J. M.: Ice detection using  
399 thermal infrared radiometry on wind turbine blades, *Measurement*, 93, 157–163,  
400 doi:10.1016/j.measurement.2016.06.064, 2016.
- 401 Hacker, J. and Neuner, G.: Ice propagation in plants visualized at the tissue level by infrared  
402 differential thermal analysis (IDTA), *Tree Physiol.*, 27(12), 1661–70,  
403 doi:10.1093/treephys/27.12.1661, 2007.
- 404 Hansman, R. J. and Dershowitz, A. L.: Method of and apparatus for detection of ice accretion,  
405 1994.
- 406 Harrison, A. D., Whale, T. F., Rutledge, R., Lamb, S., Tarn, M. D., Porter, G. C. E., Adams,  
407 M., McQuaid, J. B., Morris, G. J. and Murray, B. J.: An instrument for quantifying  
408 heterogeneous ice nucleation in multiwell plates using infrared emissions to detect freezing,  
409 *Atmos. Meas. Tech. Discuss.*, (June), 1–22, doi:10.5194/amt-2018-177, 2018.
- 410 Hartmann, S., Augustin, S., Clauss, T., Wex, H., Santl-Temkiv, T., Voigtländer, J.,  
411 Niedermeier, D. and Stratmann, F.: Immersion freezing of ice nucleation active protein  
412 complexes, *Atmos. Chem. Phys.*, 13, 5751–5766, doi:10.5194/acpd-12-21321-2012, 2013.
- 413 Häusler, T., Witek, L., Felgitsch, L., Hitzemberger, R. and Grothe, H.: Freezing on a Chip - A  
414 New Approach to Determine Heterogeneous Ice Nucleation of Micrometer-Sized Water  
415 Droplets, *Atmosphere*, 9(4), 140, doi:10.3390/atmos9040140, 2018.
- 416 Hill, T. C. J., Demott, P. J., Tobo, Y., Fröhlich-Nowoisky, J., Moffett, B. F., Franc, G. D. and  
417 Kreidenweis, S. M.: Sources of organic ice nucleating particles in soils, *Atmos. Chem. Phys.*,  
418 16, 7195–7211, doi:10.5194/acp-16-7195-2016, 2016.
- 419 Kunert, A. T., Scheel, J. F., Helleis, F., Klimach, T., Pöschl, U. and Fröhlich-Nowoisky, J.:



- 420 New High-Performance Droplet Freezing Assay (HP-DFA) for the Analysis of Ice Nuclei with  
421 Complex Composition, in EGU General Assembly Conference Abstracts, vol. 18, pp.  
422 EPSC2016-6293., 2016a.
- 423 Kunert, A. T., Scheel, J. F., Helleis, F., Klimach, T., Pöschl, U. and Fröhlich-Nowoisky, J.:  
424 TINA: A New High-Performance Droplet Freezing Assay for the Analysis of Ice Nuclei with  
425 Complex Composition, in 4th Workshop - Microphysics of Ice Clouds., 2016b.
- 426 Kunert, A. T., Lamneck, M., Gurk, C., Helleis, F., Klimach, T., Scheel, J. F., Pöschl, U. and  
427 Fröhlich-Nowoisky, J.: TINA, a new fully automated high-performance droplet freezing assay  
428 coupled to a customized infrared detection system, in EGU General Assembly Conference  
429 Abstracts, vol. 19, p. 13571., 2017a.
- 430 Kunert, A. T., Lamneck, M., Gurk, C., Helleis, F., Klimach, T., Scheel, J. F., Pöschl, U. and  
431 Fröhlich-Nowoisky, J.: TINA, a new fully automated high-performance droplet freezing assay  
432 coupled to a customized infrared detection system, in 5th Workshop - Microphysics of Ice  
433 Clouds., 2017b.
- 434 Kunert, A. T., Lamneck, M., Helleis, F., Scheel, J. F., Pöschl, U. and Fröhlich-Nowoisky, J.:  
435 TINA: Twin-plate ice nucleation assay with infrared detection for high-throughput droplet  
436 freezing experiments, in INUIT Final Conference and 2nd Atmospheric Ice Nucleation  
437 Conference., 2018.
- 438 Liu, F., Lakey, P., Berkemeier, T., Tong, H., Kunert, A. T., Meusel, H., Su, H., Cheng, Y.,  
439 Fröhlich-Nowoisky, J., Lai, S., Weller, M. G., Shiraiwa, M., Pöschl, U. and Kampf, C. J.:  
440 Atmospheric protein chemistry influenced by anthropogenic air pollutants: nitration and  
441 oligomerization upon exposure to ozone and nitrogen dioxide, *Faraday Discuss.*, 200, 413–427,  
442 doi:10.1039/C7FD00005G, 2017.
- 443 Möhler, O., Georgakopoulos, D. G., Morris, C. E., Benz, S., Ebert, V., Hunsmann, S., Saathoff,  
444 H., Schnaiter, M. and Wagner, R.: Heterogeneous ice nucleation activity of bacteria: new  
445 laboratory experiments at simulated cloud conditions, *Biogeosciences Discuss.*, 5(2), 1445–  
446 1468, doi:10.5194/bgd-5-1445-2008, 2008.
- 447 Murray, B. J. (Ben), Broadley, S. L., Wilson, T. W., Bull, S. J., Wills, R. H., Christenson, H.  
448 K. and Murray, E. J.: Kinetics of the homogeneous freezing of water, *Phys. Chem. Chem. Phys.*,  
449 12(35), 10380–7, doi:10.1039/c003297b, 2010.
- 450 O’Sullivan, D., Murray, B. J., Malkin, T. L., Whale, T. F., Umo, N. S., Atkinson, J. D., Price,  
451 H. C., Baustian, K. J., Browse, J. and Webb, M. E.: Ice nucleation by fertile soil dusts: Relative  
452 importance of mineral and biogenic components, *Atmos. Chem. Phys.*, 14(4), 1853–1867,  
453 doi:10.5194/acp-14-1853-2014, 2014.



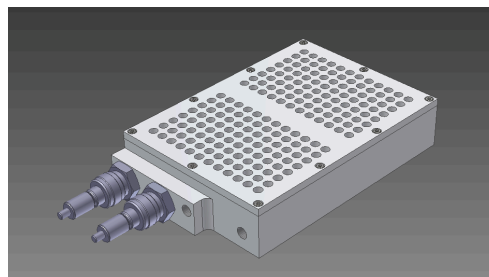
- 454 Pearce, R. S. and Fuller, M. P.: Freezing of Barley Studied by Infrared Video Thermography,  
455 *Plant Physiol.*, 125(January), 227–240, 2001.
- 456 Pruppacher, H. R. and Klett, J. D.: *Microphysics of Clouds and Precipitation*, 2nd ed., Springer  
457 Netherlands, Dordrecht., 1997.
- 458 Pummer, B. G., Budke, C., Niedermeier, D., Felgitsch, L., Kampf, C. J., Huber, R. G., Liedl,  
459 K. R., Loerting, T., Moschen, T., Schauperl, M., Tollinger, M., Morris, C. E., Wex, H., Grothe,  
460 H., Pöschl, U., Koop, T. and Fröhlich-Nowoisky, J.: Ice nucleation by water-soluble  
461 macromolecules, *Atmos. Chem. Phys.*, 15, 4077–4091, doi:10.5194/acp-15-4077-2015, 2015.
- 462 Sekozawa, Y., Sugaya, S. and Gemma, H.: Observations of Ice Nucleation and Propagation in  
463 Flowers of Japanese Pear (*Pyrus pyrifolia* Nakai) using Infrared Video Thermography, *J. Japan.*  
464 *Soc. Hort. Sci.*, 73(1), 1–6, doi:10.1248/cpb.37.3229, 2004.
- 465 Stier, J. C., Filiault, D. L., Wisniewski, M. and Palta, J. P.: Visualization of freezing progression  
466 in turfgrasses using infrared video thermography, *Crop. Sci.*, 43(1), 415–420, 2003.
- 467 Stopelli, E., Conen, F., Zimmermann, L., Alewell, C. and Morris, C. E.: Freezing nucleation  
468 apparatus puts new slant on study of biological ice nucleators in precipitation, *Atmos. Chem.*  
469 *Phys.*, 7, 129–134, doi:10.5194/amt-7-129-2014, 2014.
- 470 Tobo, Y.: An improved approach for measuring immersion freezing in large droplets over a  
471 wide temperature range, *Sci Rep*, 6(September), 32930, doi:10.1038/srep32930, 2016.
- 472 Turner, M. A., Arellano, F. and Kozloff, L. M.: Three separate classes of bacterial ice nucleation  
473 structures, *J. Bacteriol.*, 172(5), 2521–2526, 1990.
- 474 Vali, G.: Quantitative Evaluation of Experimental Results an the Heterogeneous Freezing  
475 Nucleation of Supercooled Liquids, *J. Atmos. Sci.*, 28(3), 402–409, doi:10.1175/1520-  
476 0469(1971)028<0402:QEOERA>2.0.CO;2, 1971a.
- 477 Vali, G.: Supercooling of Water and Nucleation of Ice (Drop Freezer), *Am. J. Phys.*, 39(10),  
478 1125, doi:10.1119/1.1976585, 1971b.
- 479 Ward, P. J. and DeMott, P. J.: Preliminary experimental evaluation of Snomax snow inducer,  
480 *Pseudomonas syringae*, as an artificial ice nucleus for weather modification, *J. Weather Modif.*,  
481 21(1), 9–13, 1989.
- 482 Whale, T. F., Murray, B. J., O’Sullivan, D., Wilson, T. W., Umo, N. S., Baustian, K. J.,  
483 Atkinson, J. D., Workneh, D. A. and Morris, G. J.: A technique for quantifying heterogeneous  
484 ice nucleation in microlitre supercooled water droplets, *Atmos. Meas. Tech.*, 8(6), 2437–2447,  
485 doi:10.5194/amt-8-2437-2015, 2015.
- 486 Wisniewski, M., Lindow, S. E. and Ashworth, E. N.: Observations of Ice Nucleation and  
487 Propagation in Plants Using Infrared Video Thermography, *Plant Physiol.*, 113(2), 327–334,



- 488 1997.
- 489 Wisniewski, M., Glenn, D. M., Gusta, L. and Fuller, M. P.: Using Infrared Thermography to  
490 Study Freezing in Plants, *HortScience*, 43(6), 1648–1651, 2008.
- 491 Workmaster, B.: Ice nucleation and propagation in cranberry uprights and fruit using infrared  
492 video thermography, *J. Amer. Soc. Hort.Sci.*, 124(6), 619–625, 1999.
- 493 Wright, T. P. and Petters, M. D.: The role of time in heterogeneous freezing nucleation, *J.*  
494 *Geophys. Res. Atmos.*, 118(9), 3731–3743, doi:10.1002/jgrd.503652013, 2013.
- 495 Zarogtas, D., Liolios, N. T. and Anastassopoulos, E.: Supercooling, ice nucleation and crystal  
496 growth: A systematic study in plant samples, *Cryobiology*, 72(3), 239–243,  
497 doi:10.1016/j.cryobiol.2016.03.012, 2016.

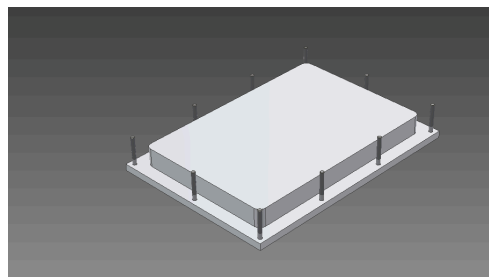


498 (a) 96-well sample holder block



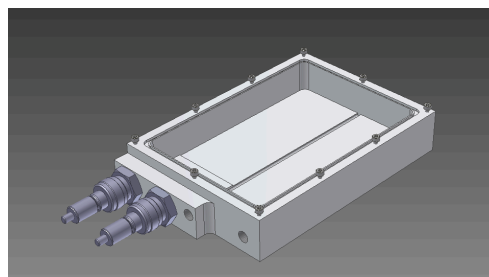
499

500 (b) 96-well top (flipped)



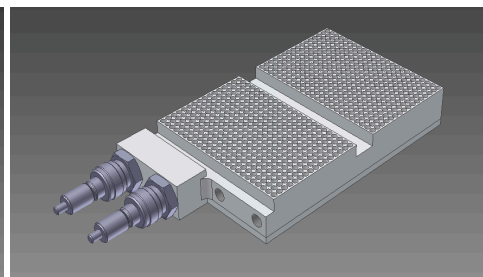
501

502 (c) 96-well bottom

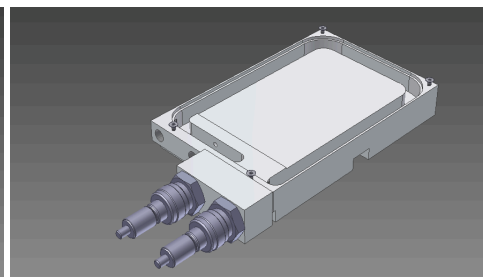


503

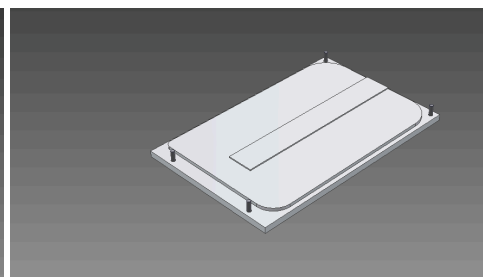
(d) 384-well sample holder block



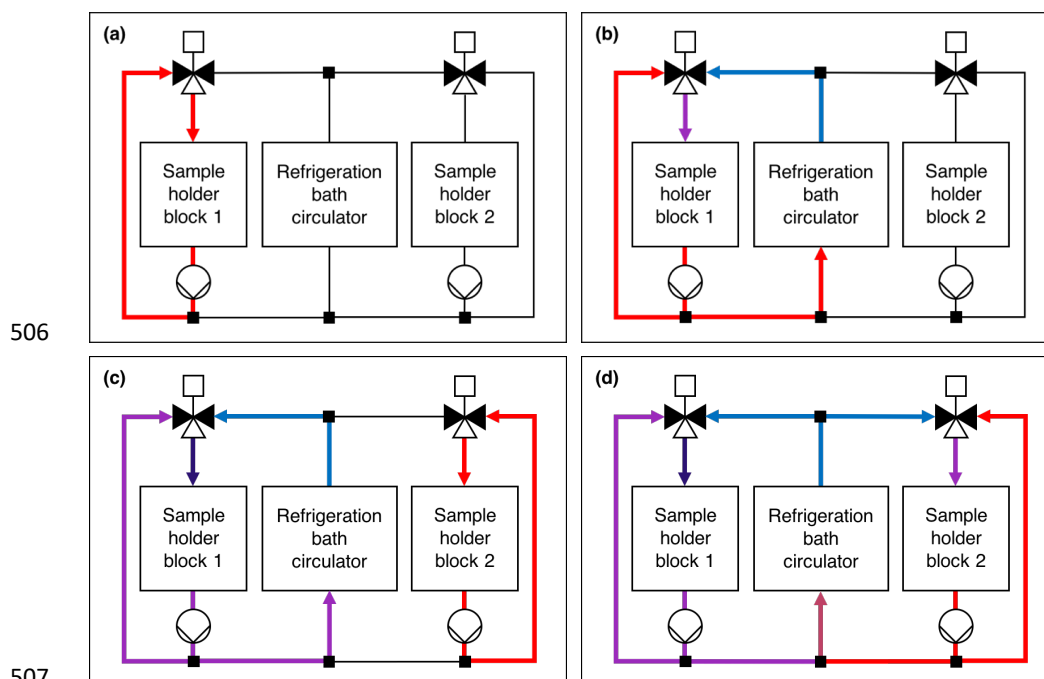
(e) 384-well top (flipped)

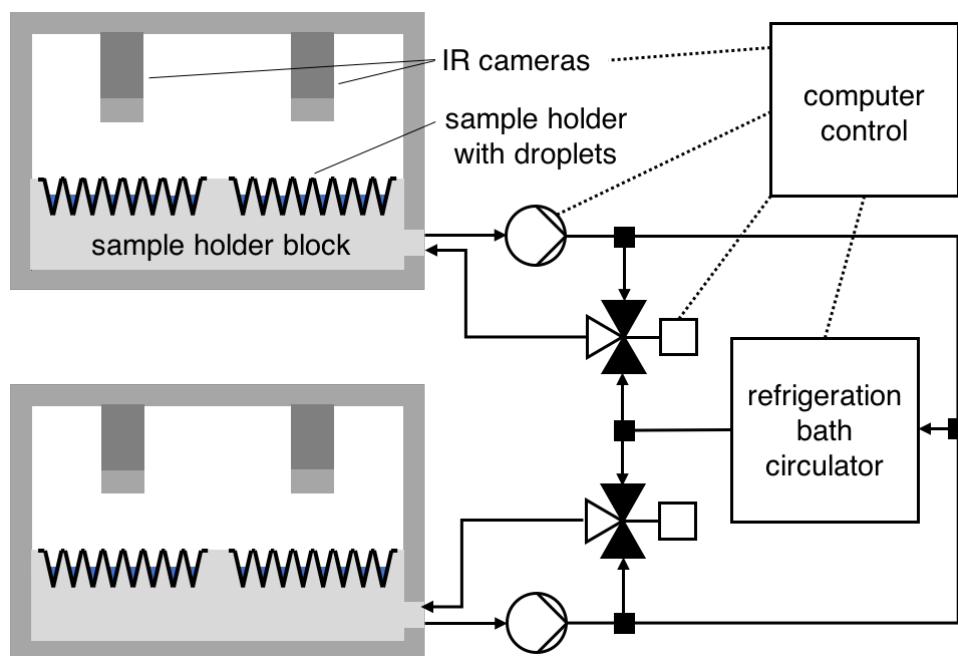


(f) 384-well bottom



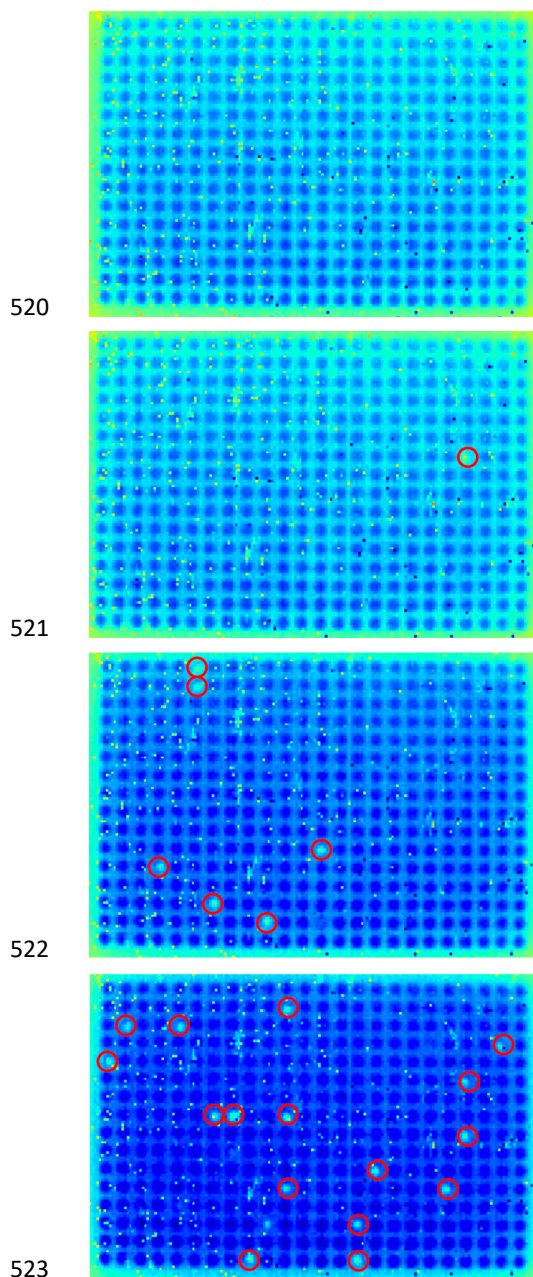
504 **Figure 1.** Sample holder and cooling blocks of the Twin-plate Ice Nucleation Assay (TINA)  
505 with (a-c) 96-well plates and (d-f) 384-well plates (CAD drawings).



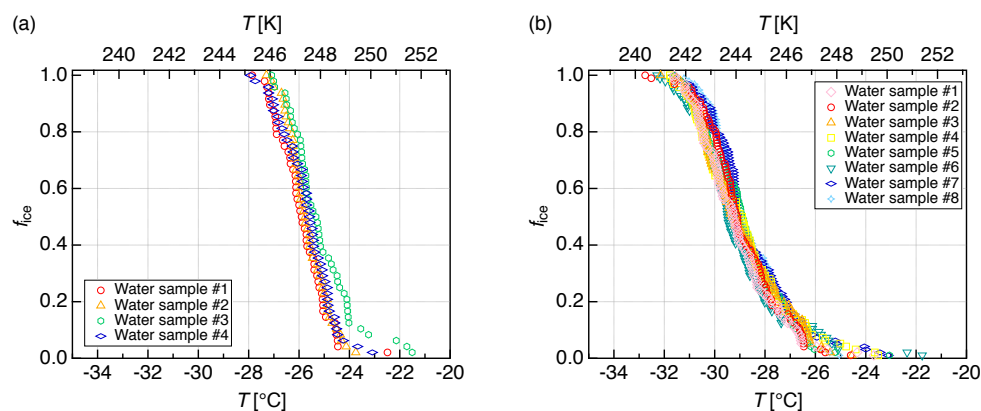


516

517 **Figure 3.** Schematic illustration of the overall setup: sample holder blocks, sample holders with  
518 droplets, IR cameras, cooling system with refrigeration bath circulator, pumps and mixing  
519 valves, computer control.

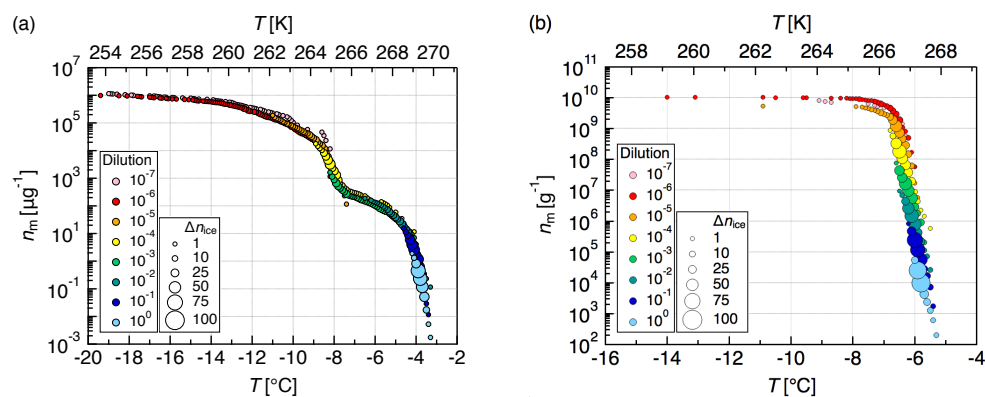


524 **Figure 4.** Sequence of infrared camera images showing 384 droplets during cooling. Red circles  
525 indicate freezing droplets.



526

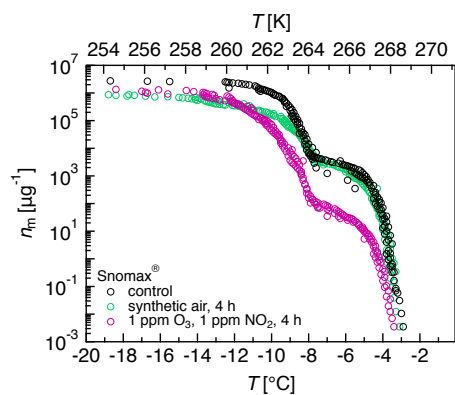
527 **Figure 5.** Freezing experiments with pure water droplets. Fraction of frozen droplets ( $f_{ice}$ ) vs.  
 528 temperature  $T$  obtained with a continuous cooling rate of  $1 \text{ K min}^{-1}$  and a droplet volume of  $3$   
 529  $\mu\text{L}$ . **(a)** Four different samples with 48 droplets each apportioned over two 96-well plates. **(b)**  
 530 Eight different samples with 96 droplets each apportioned over two 384-well plates.



531

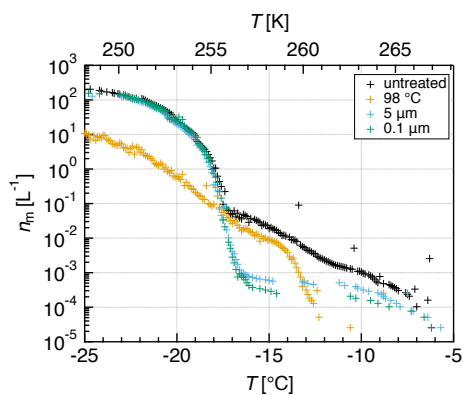
532 **Figure 6.** Measurements of dilution series of (a) bacterial IN (Snomax<sup>®</sup>) and (b) fungal IN  
533 (*Mortierella alpina* 13A). Cumulative number of IN ( $n_m$ ) per unit mass of Snomax<sup>®</sup> and  
534 mycelium, respectively, vs. temperature  $T$ . Droplets of the same dilution of three independent  
535 measurements were added to a total droplet number of 288 (3 x 96 droplets). Symbol colors  
536 indicate different dilutions; symbol size indicates the number of frozen droplets per temperature  
537 interval ( $\Delta T = 0.1$  K).

538



539

540 **Figure 7:** Freezing experiments with ozonized and nitrated bacterial IN. Cumulative number  
541 of IN ( $n_m$ ) per unit mass of Snomax<sup>®</sup> vs. temperature  $T$ . Symbol colors indicate different  
542 exposure conditions.



543

544 **Figure 8.** Freezing experiments with aqueous extracts of atmospheric aerosols. Number of IN  
545 per liter air vs. temperature  $T$  for untreated (black), heated (orange),  $5\ \mu\text{m}$  filtered (blue), and  
546  $0.1\ \mu\text{m}$  filtered (green) filter extracts. Data of different dilutions were averaged for each  
547 treatment.